

# Determining $\alpha$ -Helical and $\beta$ -Sheet Secondary Structures via Pulsed Electron Spin Resonance Spectroscopy

Andy Zhou, Shadi Abu-Baker, Indra D. Sahu, Lishan Liu, Robert M. McCarrick, Carole Dabney-Smith, and Gary A. Lorigan\*

Department of Chemistry and Biochemistry, Miami University, Oxford, Ohio 45056, United States

**ABSTRACT:** A new method has been developed to determine  $\alpha$ -helical and  $\beta$ -sheet secondary structural components of aqueous and membrane-bound proteins using pulsed electron paramagnetic resonance (EPR) spectroscopy. The three-pulse electron spin echo envelope modulation (ESEEM) technique was used to detect weakly coupled  $^2\text{H}$ -labeled nuclei on side chains in the proximity of a strategically placed nitroxide spin-label up to 8 Å away. Changes in the ESEEM spectra for different samples correlate directly to periodic structural differences between  $\alpha$ -helical and  $\beta$ -sheet motifs. These distinct trends were demonstrated with  $\alpha$ -helical (M2 $\delta$  subunit of the acetylcholine receptor) and  $\beta$ -sheet (ubiquitin) peptides in biologically relevant sample environments.

Limited structural information exists for membrane proteins and thus it is essential for new biophysical techniques to be developed and refined. For the first time, a method for probing the secondary structure using electron spin echo envelope modulation (ESEEM) spectroscopy has been applied to distinguish between  $\alpha$ -helical and  $\beta$ -sheet peptides. Our previous work demonstrated the determination of an  $\alpha$ -helical secondary structure using ESEEM spectra by detecting changes in dipolar couplings between a nitroxide spin label and nearby deuterated side chains of  $\alpha$ -helical peptides.<sup>1</sup> Application of this technique to  $\beta$ -sheet peptides provides complementary results which assist to establish ESEEM spectroscopy as a strong structural determination tool.<sup>2,3</sup> Structural information can be obtained using micromolar concentrations of sample with short data acquisition times in membrane protein systems that often prove difficult to study using traditional structural techniques such as solution nuclear magnetic resonance (NMR) and X-ray crystallography owing to size limitations ( $\leq 50$  kDa), low-yield overexpression, and low quality crystals.<sup>2,4,5</sup>

Previously, the  $\alpha$ -helical content of the M2 $\delta$  subunit of the acetylcholine receptor was mapped using this ESEEM technique by fixing a  $^2\text{H}$ -labeled Val ( $d_8$ ) at position 15 ( $i$ ), and varying the (1-oxyl-2,2,5,5-tetramethyl-3-pyrroline-3-methyl) methanesulfonate (MTSL) spin label at four successive positions ( $i+1$  through  $i+4$ ).<sup>1</sup> Three-pulse ESEEM was performed in order to detect weakly coupled  $^2\text{H}$  atoms on the side chain within  $\sim 8$  Å of the nitroxide spin label.<sup>6,7</sup> The time domain ESEEM spectrum for a peptide construct displayed a distinct  $^2\text{H}$  Larmor modulation pattern when the spin label was within the 8 Å detection limit. Given these four constructs, it was clear that the  $\alpha$ -helical periodicity was best demonstrated between the  $i+2$  and  $i+3$  constructs, where  $^2\text{H}$

modulation was absent in the  $i+2$  sample and present in the  $i+3$  sample.<sup>1</sup> Through these results, the 3.6 residue/turn periodicity of the  $\alpha$ -helix translated to spectroscopically discernible distance changes between the labeled sites of  $i+2$  and  $i+3$  constructs. This exact labeling paradigm can be applied to an ideal  $\beta$ -sheet peptide and probed via the ESEEM technique to provide both novel and complementary results to the previous M2 $\delta$  helix data. In addition, applying this technique to a water-soluble  $\beta$ -sheet peptide in contrast to the membrane bound M2 $\delta$  helical peptide demonstrates the feasibility of this technique in aqueous environments as well as the membrane mimicking bicelle environment previously demonstrated.<sup>1</sup> A solution-NMR characterized  $\beta$ -sheet peptide composed of the first 17 residues of ubiquitin and the  $\alpha$ -helical M2 $\delta$  subunit of the acetylcholine receptor were used as ideal secondary structures for  $i+2$  and  $i+3$  labeling using a  $^2\text{H}$ -labeled  $d_{10}$  leucine.<sup>8,9</sup>  $^2\text{H}$ -labeled  $d_{10}$  Leu was placed at position 15 for the M2 $\delta$  peptide and position 17 for the ubiquitin peptide. A nitroxide spin label (MTSL) was placed two or three residues away (denoted  $i+2$  and  $i+3$ ) via site-directed spin labeling.<sup>8,10,11</sup> CD spectroscopy, molecular modeling, and molecular dynamics studies were also performed on all M2 $\delta$  and ubiquitin peptide samples to ensure ideal holistic sample integrity and to estimate distances between the spin label and  $^2\text{H}$  nuclei on the leucine side chain.

Both M2 $\delta$  and ubiquitin peptide constructs were synthesized on a CEM microwave assisted peptide synthesizer using Fmoc protection chemistry.<sup>12</sup> A solution of deuterated  $d_{10}$  Leu (Isotec) dissolved in *N*-methyl-2-pyrrolidone was used as the deuterated residue substitution. The peptides were cleaved from their resin support and purified via high performance liquid chromatography (HPLC) as previously described.<sup>10</sup> The purified peptides were subsequently labeled with *S*-(2,2,5,5-tetramethyl-2,5-dihydro-1H-pyrrol-3-yl)methyl methanesulfonothioate (MTSL) spin label at 10 $\times$  molar excess in 500  $\mu\text{L}$  of dimethyl sulfoxide (DMSO). Reaction products were repurified using HPLC as described.<sup>10</sup> The peptides were confirmed to be over 95% pure by MALDI-TOF mass spectrometry. M2 $\delta$  peptides were incorporated into dimyristoyl-phosphatidylcholine (DMPC)/dihexanoyl-phosphatidylcholine (DHPC) (3.5/1) lipid bicelles at a 500:1 lipid/protein ratio. The ubiquitin peptide was dissolved in an aqueous buffer using a standard protocol.<sup>9</sup>

Three-pulse ESEEM measurements were performed on a Bruker ELEXSYS E580 spectrometer equipped with an MS3

Received: August 9, 2012

Revised: September 10, 2012

Published: September 11, 2012



split ring resonator. The measurements were conducted at 80 K at a microwave frequency of 9.269 GHz with 16 ns  $\pi/2$  pulse widths. A starting  $T$  of 368 ns and 512 points in 12 ns increments were used for all samples. A  $\tau$  value of 200 ns was chosen to suppress proton modulation. Sample volumes were approximately 40  $\mu$ L. M2 $\delta$  bicelles and aqueous ubiquitin peptide samples were analyzed using a Jasco J-810 spectropolarimeter over a wavelength range of 190–250 nm. Concentrations range from 0.01 to 0.1 mg/mL protein.

The CD spectrum of  $i+3$  ubiquitin construct in Figure 1 shows a large and broad negative band centered at 218 nm

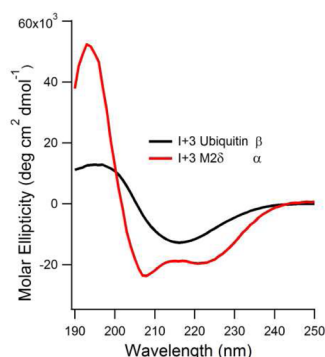


**Figure 1.** CD spectra of  $i+3$  M2 $\delta$  and ubiquitin construct in DMPC/DHPC bicelles with a lipid/protein ratio of 200:1 at 298 K and pH 7.

indicating  $\beta$ -sheet secondary structure. The M2 $\delta$  CD spectrum indicates a  $\alpha$ -helical secondary structure through the two negative bands at 222 nm and 208 nm.

Molecular modeling and molecular dynamics studies for each sample were performed using nanoscale molecular dynamics (NAMD) with the molecular graphics software VMD in the similar way reported in the literature.<sup>1,13,14</sup> The structures of the AChR M2 $\delta$  peptide and ubiquitin peptide were obtained from the Protein Data Bank (PDB entry: 1EQ8 for M2 $\delta$  peptide and 1EQQ for ubiquitin peptide). Cysteine mutants were created at the  $i+2$  and  $i+3$  positions using VMD. The MTSL nitroxide spin probe was attached by using CHARMM force-field topology files incorporated in NAMD. Molecular dynamic simulations were collected out to 1 ns at room temperature using Langevin dynamics under NAMD. This time scale corresponds to the MTSL and Leu side chain dynamics. The trajectory data were recorded in 1 ps increments. The possible distance distribution for each deuterium and SL was obtained from the analysis of the data in VMD.

Figure 2 shows three-pulse ESEEM data for  $i+2$  and  $i+3$  for both M2 $\delta$  and ubiquitin peptide constructs. In Figure 2A, the presence of  $^2\text{H}$  modulation and a corresponding FT peak at the  $^2\text{H}$  Larmor frequency in the  $i+2$  ubiquitin spectrum indicates weak dipolar coupling between deuterium nuclei and the spin label, thus indicating that the distance between the  $^2\text{H}$  nuclei on Leu and the spin labels must be less than the  $\sim 8$  Å detection limit. The absence of  $^2\text{H}$  modulation in the  $i+3$  ubiquitin sample implies that the  $^2\text{H}$ -SL distances are greater than 8 Å. The ESEEM results indicate that for ideal  $\beta$ -sheet secondary structure peptides, the radial distance between the  $d_{10}$  Leu side chain and nitroxide spin label surpasses the 8 Å detection limit as we shift from  $i+2$  to  $i+3$ , and for the first time this shift in distance is detectable on  $\beta$ -sheets with ESEEM spectroscopy. This distance shift is caused by the MTSL and the  $d_{10}$  Leu side chain pointing toward the same side of the  $\beta$ -sheet in  $i+2$

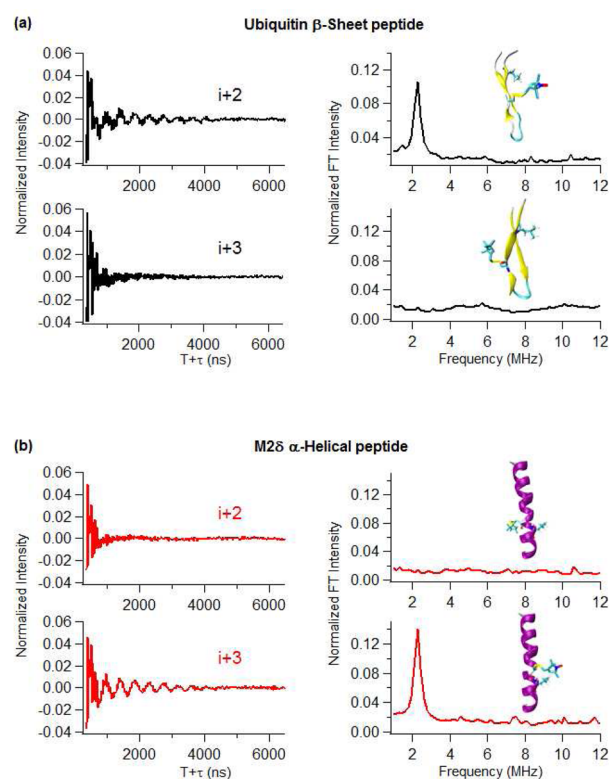


**Figure 2.** (a, b) Normalized time and FT frequency domain data for the peptide constructs from three-pulse ESEEM experiments. M2 $\delta$  peptides were embedded in DMPC/DHPC lipid bicelles. Ubiquitin peptides were dissolved in water. The inset structural pictures show the location of the spin label and the  $^2\text{H}$ -labeled Leu.

constructs to opposing sides in  $i+3$  constructs. This shift is visualized by the illustrations embedded in Figure 2A. Figure 2B shows the ESEEM data for the M2 $\delta$  peptide. Conversely, the M2 $\delta$   $i+2$  spectrum does not reveal any  $^2\text{H}$  modulation, whereas the M2 $\delta$   $i+3$  spectrum does. For M2 $\delta$ , the radial distance between the  $d_{10}$  Leu side chain and nitroxide spin label diminishes into the 8 Å limit when shifting from  $i+2$  to  $i+3$ . Visually, the MTSL and  $D_{10}$  Leu side chain point toward opposite sides of the helix in  $i+2$  constructs and wrap around to point toward the same side of the helix in  $i+3$  constructs similar to the illustrations in Figure 2B. The complementary results of  $i+2/i+3$  spectra for  $\alpha$  helices and  $\beta$  sheets attained through this novel ESEEM approach establish a simple qualitative method for determining site-specific secondary structure of any given protein system.

To support the data, molecular modeling and molecular dynamics studies were conducted to estimate distances between the  $^2\text{H}$  nuclei on the Leu  $d_{10}$  side chain and the N–O bond on the SL for  $i+2$  and  $i+3$  samples of both peptides.  $^2\text{H}$ -SL distances (9–15 Å) for  $i+3$  ubiquitin sample and (11–17 Å) for the  $i+2$  M2 $\delta$  sample were found to be outside the ESEEM detection range of 8 Å. Conversely,  $^2\text{H}$ -SL distances for the (5–10 Å) for the  $i+2$  ubiquitin sample and (4–10 Å) for the  $i+3$  M2 $\delta$  sample were found to be within the ESEEM detection range though with differing distance distributions.

This novel biophysical technique for secondary structure determination is analogous to solid-state NMR techniques such as rotational echo double resonance (REDOR), which measures dipolar couplings between NMR active nuclei.<sup>15–17</sup> These measurements are coupled with spectral simulations to

gain information about protein structure. However, poor signal-to-noise requires that these experiments be performed with milligram amounts of isotopically labeled protein and long data acquisition times that can take weeks to collect. In comparison, this ESEEM approach requires microgram amounts of protein sample, and high-quality spectra of specific targeted sites were attained within minutes. This technique also opens up the possibility of gleaned quantitative distance information in addition to the qualitative data described in this study. For instance, an amino acid side chain with fewer  $^2\text{H}$  labeled nuclei could afford the possibility of determining the distance between the nuclei and the MTSL label based on the  $r^{-6}$  dependence on the modulation depth.<sup>18</sup> Difficulties can occur when dealing with MTSL dynamics and multiple side-chain conformations of Leu. From the literature, both MTSL and Leu side chain have multiple torsional angle rotations in their structures.<sup>19–22</sup> Because of these rotational freedoms, the experiments performed at 80 K capture MTSL and Leu in a variety of conformations resulting in a broadening of distance distributions between MTSL and deuterons.<sup>19,23,24</sup> NMR or X-ray crystallography can provide higher resolution structural data when compared with this technique, but with more time and effort and still not optimal for membrane proteins. However, this ESEEM technique provides qualitative and site-specific secondary structure information to be gathered without the requirement for high concentration samples or crystallization and in a much shorter time. Other EPR-based techniques such as the nitroxide scanning and power saturation EPR can probe secondary structure through analysis of data from multiple constructs.<sup>11,25</sup> However, this ESEEM approach only requires two constructs to establish secondary structure and directly probes distances between the residues that conform to a given structure.

The results presented in this work clearly demonstrate that  $\alpha$ -helices and  $\beta$ -sheets can be spectroscopically discerned through their distinct  $i+2$  and  $i+3$  ESEEM spectra in both membrane mimicking and aqueous systems. This approach can also be applied to larger protein systems by overexpression in an appropriate eukaryotic or prokaryotic protein expression system using a minimal growth medium supplemented with a  $^2\text{H}$ -labeled amino acid such as Leu. This technique would result in all Leu residues in the protein being deuterated. Secondary structural components would be identified with ESEEM data in a similar fashion as outlined in this work at the  $i+2$  or  $i+3$  positions. However, the spin label would need to be strategically placed to avoid areas with multiple Leu residues. This approach allows the secondary structure in a particular region of a much larger protein to be probed using this ESEEM method. Combined with an appropriate native deuterated probe and a strategically placed MTSL, this ESEEM approach can detect short-range distances ( $<8$  Å) between specific sites on large membrane protein complexes, determine the secondary structure of different protein segments, and investigate protein–protein interactions.

## AUTHOR INFORMATION

### Corresponding Author

\*E-mail: gary.lorigan@miamioh.edu. Phone: (513) 529-3338.

### Notes

The authors declare no competing financial interest.

## ACKNOWLEDGMENTS

This work was accomplished thanks to the National Institute of Health Grant R01GM080542 and a National Science Foundation Award CHE-1011909. The pulsed EPR spectrometer was purchased through the NSF and the Ohio Board of Regents grants (MRI-0722403). The mass spectrometer was purchased using an NSF (CHE-0839233) grant.

## REFERENCES

- (1) Mayo, D., Zhou, A., Sahu, I., McCarrick, R., Walton, P., Ring, A., Troxel, K., Coey, A., Hawn, J., Emwas, A. H., and Lorigan, G. A. (2011) *Protein Sci.* 20, 1100–1104.
- (2) Bordag, N., and Keller, S. (2010) *Chem. Phys. Lipids* 163, 1–26.
- (3) McLuskey, K., Roszak, A. W., Zhu, Y., and Isaacs, N. W. (2010) *Eur. Biophys. J.* EBF 39, 723–755.
- (4) Alexander, N., Bortolus, M., Al-Mestarihi, A., Mchaourab, H., and Meilerl (2008) *J. Structure* 16, 181–195.
- (5) Huang, C., and Mohanty, S. (2010) *J. Am. Chem. Soc.* 132, 3662–3663.
- (6) Lorigan, G. A., Britt, R. D., Kim, J. H., and Hille, R. (1994) *Biochem. Biophys. Acta* 1185, 284–294.
- (7) Milov, A. D., Samoilova, R. I., Shubin, A. A., Gorbunova, E. Y., Mustaeva, L. G., Ovchinnikova, T. V., Raap, J., and Tsvetkov, Y. D. (2010) *Appl. Magn. Reson.* 38, 75–84.
- (8) Kim, J., and McNamee, M. G. (1998) *Biochemistry* 37, 4680–4686.
- (9) Zerella, R., Chen, P. Y., Evans, P. A., Raine, A., and Williams, D. H. (2000) *Protein Sci.* 9, 2142–2150.
- (10) Inbaraj, J. J., Cardon, T. B., Laryukhin, M., Grosser, S. M., and Lorigan, G. A. (2006) *J. Am. Chem. Soc.* 128, 9549–9554.
- (11) Klug, C. S., and Feix, J. B. (2008) *Methods Cell Biol.* 84, 617–658.
- (12) Oblant-Montal, M., Buhler, L., Iwamoto, T., Tomich, J., and Montal, M. (1993) *J. Biol. Chem.* 268, 14601–14607.
- (13) Humphrey, W., Dalke, A., and Schulten, K. (1996) *J. Mol. Graph.* 14, 33–38.
- (14) Phillips, J. C., Braun, R., Wang, W., Gumbart, J., Tajkhorshid, E., Villa, E., Chipot, C., Skeel, R. D., Kale, L., and Schulten, K. (2005) *J. Comput. Chem.* 26, 1781–1802.
- (15) Chu, S. D., Coey, A. T., and Lorigan, G. A. (2010) *Biochem. Biophys. Acta - Biomembranes* 1798, 210–215.
- (16) Howell, S. C., Mesleh, M. F., and Opella, S. (2005) *J. Biochemistry* 44, 5196–5206.
- (17) Liu, W., Fei, J. Z., Kawakami, T., and Smith, S. O. (2007) *Biochem. Biophys. Acta* 1768, 2971–2978.
- (18) Mims, W. B. (1972) *Phys. Rev. B-Solid State* 5, 2409–2419.
- (19) Batchelder, L., Sullivan, C., Jelinski, L., and Torchia, D. (1982) *Biophysics* 79, 386–389.
- (20) Beier, C., and Steinhoff, H. (2006) *Biophys. J.* 91, 2647–2664.
- (21) Columbus, L., and Hubbell, W. L. (2002) *Trends Biochem. Sci.* 27, 288–295.
- (22) Sezer, D., Freed, J. H., and Roux, B. (2008) *J. Phys. Chem. B* 112, 5755–5767.
- (23) Fanucci, G. E., and Cafiso, D. S. (2006) *Curr. Opin. Struct. Biol.* 16, 644–653.
- (24) McHaourab, H. S., Lietzow, M. A., Hideg, K., and Hubbell, W. L. (1996) *Biochemistry* 35, 7692–7704.
- (25) Isas, J. M., Langen, R., Haigler, H. T., and Hubbell, W. L. (2002) *Biochemistry* 41, 1464–1473.